Van der Waals Heteroepitaxial Growth of Monolayer Sb in a Puckered Honeycomb Structure

Zhi-Qiang Shi, Huiping Li, Qian-Qian Yuan, Ye-Heng Song, Yang-Yang Lv, Wei Shi, Zhen-Yu Jia, Libo Gao, Yan-Bin Chen, Wenguang Zhu, and Shao-Chun Li**

Atomically thin 2D crystals have gained tremendous attention owing to their potential impact on future electronics technologies, as well as the exotic phenomena emerging in these materials. Monolayers of α-phase Sb (α-antimonene), which shares the same puckered structure as black phosphorous, are predicted to be stable with precious properties. However, the experimental realization still remains challenging. Here, high-quality monolayer α-antimonene is successfully grown, with the thickness finely controlled. The α-antimonene exhibits great stability upon exposure to air. Combining scanning tunneling microscopy, density functional theory calculations, and transport measurements, it is found that the electron band crossing the Fermi level exhibits a linear dispersion with a fairly small effective mass, and thus a good electrical conductivity. All of these properties make the α-antimonene promising for future electronic applications.

Spurred by their prospect in electronic technologies, 2D crystals have been attracting increasing attentions. As the thickness is decreased down to the single-layer limit, 2D crystals usually exhibit different electronic properties from their bulk counterparts.[1] Exotic phenomena are also expected in single-layered materials, such as the quantum spin Hall effect,[2–6] 2D superconductivity,[7,8] charge density wave,[9–12] or magnetism.[13,14] Following the discovery of graphene,[15,16] black phosphorus (BP) has been revived as a potential candidate for optoelectronics and field-effect transistor (FET) applications,[17–20] which, however, is suffering from chemical instability. Many monoelement single-layered materials have been predicted and realized, such as Si,[21–23] Ge,[24,25] Sn,[26] B,[27,28] Hf,[29] and Te,[30] but few of them share the same crystal structure as BP.

It is believed that BP-structured monolayer (α-allotrope) can be formed in other group V elements, such as Bi (bismuthene), Sb (antimonene), or As (arsenene), and many theoretical efforts have been made to predict their structures and properties.[31–37] Comparing to their β-allotrope of hexagonal honeycomb structure that has been widely studied experimentally,[38–44] it still remains challenging to fabricate the large-scale and high-quality monolayer α-allotrope of these group V monoelements,[36] even though small patches of the α-allotrope has been observed in some mixed structures.[45]

In this study, we successfully synthesize the large-scale and high-quality α-antimonene with puckered BP structure on the T_d-WTe_2 substrate, by using molecular beam epitaxy (MBE). In our experiment, the thickness of BP-structured antimonene can be well controlled in a layer-by-layer fashion. Owing to the high quality and large scale of the Sb monolayer, it becomes possible to map the electronic band structure via quasiparticle interference (QPI) with scanning tunneling microscopy (STM). The α-antimonene exhibits a hole-doped nature with a linearly dispersed band crossing the Fermi level and a high electrical

Z.-Q. Shi, Q.-Q. Yuan, Y.-H. Song, W. Shi, Z.-Y. Jia, Prof. L. Gao, Prof. Y. B. Chen, Prof. S.-C. Li
National Laboratory of Solid State Microstructures School of Physics
Nanjing University
Nanjing 210093, China

E-mail: scli@nju.edu.cn
H. Li, Prof. W. Zhu
International Center for Quantum Design of Functional Materials (ICQD)
Hefei National Laboratory for Physical Sciences at the Microscale, and Synergetic Innovation Center of

Quantum Information and Quantum Physics
University of Science and Technology of
China Hefei, Anhui 230026, China
E-mail: wgzhu@ustc.edu.cn



The ORCID identification number(s) for the author(s) of this article can be found under https://doi.org/10.1002/adma.201806130.

DOI: 10.1002/adma.201806130

H. Li, Prof. W. Zhu
Key Laboratory of Strongly-Coupled Quantum Matter Physics
Chinese Academy of Sciences
School of Physical Sciences
University of Science and Technology of China
Hefei, Anhui 230026, China

Dr. Y.-Y. Lv
National Laboratory of Solid State Microstructures
Department of Materials Science and Engineering
Nanjing University
Nanjing 210093, China

Prof. S.-C. Li
Collaborative Innovation Center of Advanced Microstructures
Nanjing University
Nanjing 210093, China

 © 2018 WILEY-VCH Verlag GmbH & Co. KGaA, Weinheim

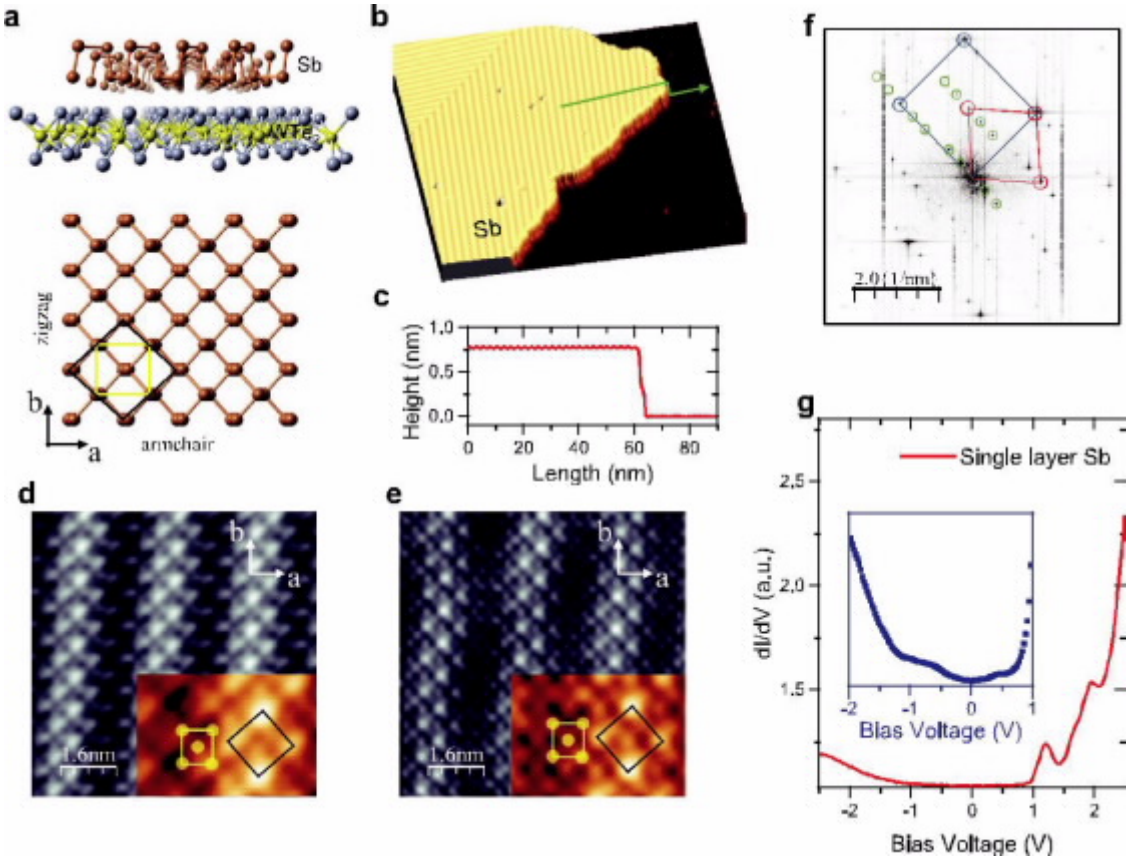


Figure 1. STM and STS results of the epitaxial single-layered α-antimonene grown on T_d-WTe_2. a) The upper is the schematic of epitaxial α-Sb on T_d-WTe_2. The lower is the top view of freestanding α-antimonene, the 1 1 and R2 unit cells are marked by yellow and black rectangles, respectively. The armchair and zigzag directions are labeled. b) The STM topology image (120 120 nm^2) of single layer α-Sb fabricated on WTe_2. U 2 V, I_t 100 pA. c) The line-scan profile taken along the green arrowed line in (b). d,e) Atomically resolved STM images (8 8 nm^2) taken at U 300 mV and U −50 mV, respectively. I_t 100 pA. In the inset, the black and yellow rectangles mark the unit cells of R2 reconstruction and 1 1 lattice. f) Fast Fourier transform (FFT) of the large-scale STM topology image, the blue, red, and green circles mark the Bravais vectors of 1 1, R2 reconstruction, and moiré pattern, respectively. g) The red curve shows the experimental STS of single layer α-Sb from −2.5 to 2.5 V. The blue curve is the enlarged part from −2.0 to 1.0 V.

conductivity. Moreover, the α-antimonene is ultrastable upon exposure to air, thus making it a good complementary to the family of 2D materials, and should be of potential to many applications.

Freestanding α-antimonene takes a distorted BP structure, consisting of two subatomic layers, as illustrated in **Figure 1**a. The antimonene layers are stacked along the vertical direction by van der Waals interaction to form the bulk antimony.[34] To achieve the nearly freestanding epitaxial α-antimonene monolayer, the substrate is required to be chemically inert and weakly bonded to suppress the hybridization to the epitaxial layer. T_d-WTe_2 is a suitable substrate to grow α-antimonene because 1) the surface is relatively inert and 2) the rectan-gular unit cell of T_d-WTe_2 surface is compatible to that of α-antimonene, as shown in Figure 1a.

Initially, Sb on the T_d-WTe_2 surface prefers a monolayer growth mode. Figure 1b shows the topographic image taken on a surface with ≈0.3 ML Sb on the T_d-WTe_2, where Sb forms the atomically flat islands with no detectable defects. The step height of the Sb island, as plotted in Figure 1c, is ≈0.78 nm, slightly larger than the calculated thickness of 0.61 nm for the single-layer antimonene film.[34] A moiré pattern, can be identified in Figure 1b as the ridge-like feature with a period of ≈2.5 nm, which is ascribed to the interference between the subtly different lattice periodicity of antimonene and T_d-WTe_2. Through optimizing the growth parameters, the single-layered film of antimonene can be grown as large as a micrometer, (see Figure S1, Supporting Information). The single-layered island is usually composed of two domains, with the orienta-tion of the moiré pattern rotated by ≈80 with respect to each other, (as shown in Figure S2, Supporting Information). The atomic-resolution STM images (Figure 1d,e), as well as the fast Fourier transform (Figure 1f), clearly reveal a reconstructed $\sqrt{2}$ $2\sqrt{}$(R2) lattice as marked by the black squares, and the original 1 1 lattice as marked by the yellow squares. The a and b axes of the 1 1 unit cell are experimentally determined to be ≈0.44 and ≈0.48 nm, very close to the calculated values for the freestanding monolayer Sb.[34] However, the original rectangular lattices are slightly distorted with an angle of ≈91 . In both domains, the moiré pattern is nearly parallel to the armchair direction of the antimonene lattice. It is worthwhile noting that the lattice constants for the 2 2 unit cell of α-$\sqrt{}$-$\sqrt{}$antimonene is 0.62 0.63 nm, closely compatible with the size of two unit cells of the substrate WTe_2, i.e., 0.63 0.68 nm,

© 2018 WILEY-VCH Verlag GmbH & Co. KGaA, Weinheim

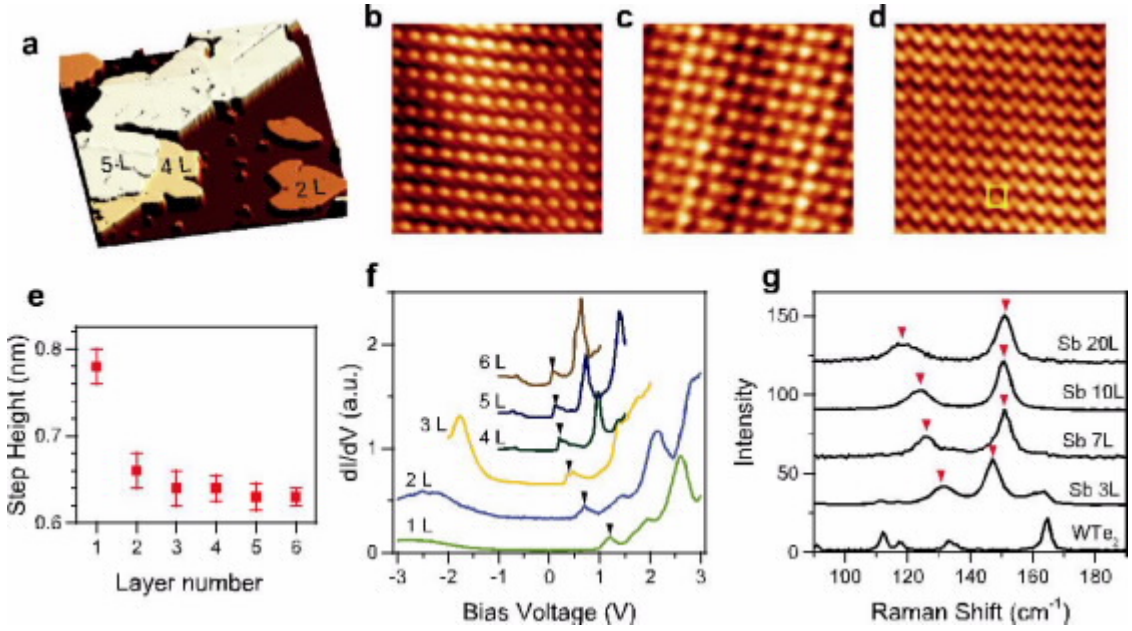


Figure 2. Characterization of the epitaxial multilayered α-antimonene grown on WTe_2. a) The STM topographic image (200 200 nm^2) of multilayered α-antimonene with thickness varying from 2 to 5L. U 2 V, I_t 100 pA. b–d) Atomically resolved STM images (5 5 nm^2) obtained on the 2, 3, and 4L, respectively. U 10 mV, I_t 100 pA. The 1 1 unit cell is marked by the yellow rectangle. e) The step height measured on the α-antimonene films of various thickness. f) Thickness-dependent STS taken on the antimonene films from 1 to 6L. The characteristic feature in the unoccupied state is marked by black triangles in each spectrum. The spectra are offset along vertical direction for clarity. g) Raman spectra taken on the bare WTe_2 and α-antimonene films with thickness of ≈3, ≈7, ≈10, and ≈20 L, respectively. The spectra are offset along vertical direction for clarity.

(see Figure S3, Supporting Information). Based on these measurements, a structural model of a 2 2 $\sqrt{}$ reconstructed antimonene on WTe_2 is proposed (as shown in Figure S2, Sup-porting Information).

The dI/dV spectra, which represent the local density of state, are taken on the terrace of the single-layer antimonene, and shown in Figure 1g. The finite density at the Fermi energy indicates a metallic nature. In fact, the dI/dV spectra are rather uniform along the surface (see Figure S4, Supporting Informa-tion), suggesting the high film quality and homogeneous elec-tronic band structure. Furthermore, the dI/dV spectra taken on different domains show subtle difference as well, (as shown in Figure S4, Supporting Information).

By increasing the amount of Sb, multilayered antimonene of large scale can be grown, as shown in **Figure 2**a. Figure 2b–d shows the atomic resolution images taken on the different layers of antimonene, confirming the BP-like puckered struc-ture for all the thickness. The step heights measured on the antimonene films from 1st to 6th layer are plotted in Figure 2e (see also Figure S5, Supporting Information). The step heights from the 2nd to the 6th layer are kept nearly constant varying from ≈0.65 to ≈0.63 nm, but smaller than the height of the 1st layer, indicating again the weak coupling between antimonene and the T_d-WTe_2 substrate. dI/dV spectra are also measured on these multiple layers, as plotted together in Figure 2f. All the dI/dV spectra exhibit the same metallic nature. The character-istic peaks in the unoccupied states, as marked by the black tri-angles in Figure 2f, gradually shift toward the Fermi energy as the thickness increases.

Raman characterization is performed on the α-antimonene films, as shown in Figure 2g. According to the density functional theory (DFT) calculation,[34] the characteristic peak at ≈147 cm^{-1} is related to the out-of-plane mode A_1^3 (147 cm^{-1} for 1st layer α-Sb), and the one at 131 cm^{-1} to the in-plane mode A_1^2 (132 cm^{-1} for 1st layer α-Sb), respectively. As the thickness increases, the A_1^2 mode at 131 cm^{-1} prominently shifts to 118 cm^{-1} (red shift), while the A_1^3 mode at 147 cm^{-1} shifts to 150 cm^{-1} (blue shift). Such Raman shifts can be ascribed to the stacking induced structural change or the anisot-ropy of the BP-like lattice, similar to what has been observed in black phosphorene and MoS_2.[18,46–48] In contrast to the BP-type Bi(110)/HOPG islands which undergo a structural transition at 4 MLs,[36] the multilayered antimonene always preserves the BP-like structure, and no structural transition is observed. In our STM measurement, the limit of thickness explored is six layers. Raman characterization indicates that the antimonene film keeps the BP-puckered structure at least up to ≈20 layers (Figure 2g).

The DFT-calculated band structure of the antimonene-WTe_2 heterostructure (Figure S6, Supporting Information) reveals that the epitaxial antimonene is hole doped, due to the elec-tron transfer from the antimonene to the underlying WTe_2 substrate and as the thickness of Sb increases, the Fermi level gradually shifts upward. Such effects can be confirmed in the following QPI analysis. Regardless of downward shift of the Fermi level, the calculated band structure of the epitaxial antimonene is overall similar with that of the freestanding antimonene, (as shown in Figure S7, Supporting Information), due to the weak interlayer coupling between the antimonene and WTe_2 substrate. Therefore, we will use the band structures of freestanding antimonene in the following discussions for simplicity.

© 2018 WILEY-VCH Verlag GmbH & Co. KGaA, Weinheim

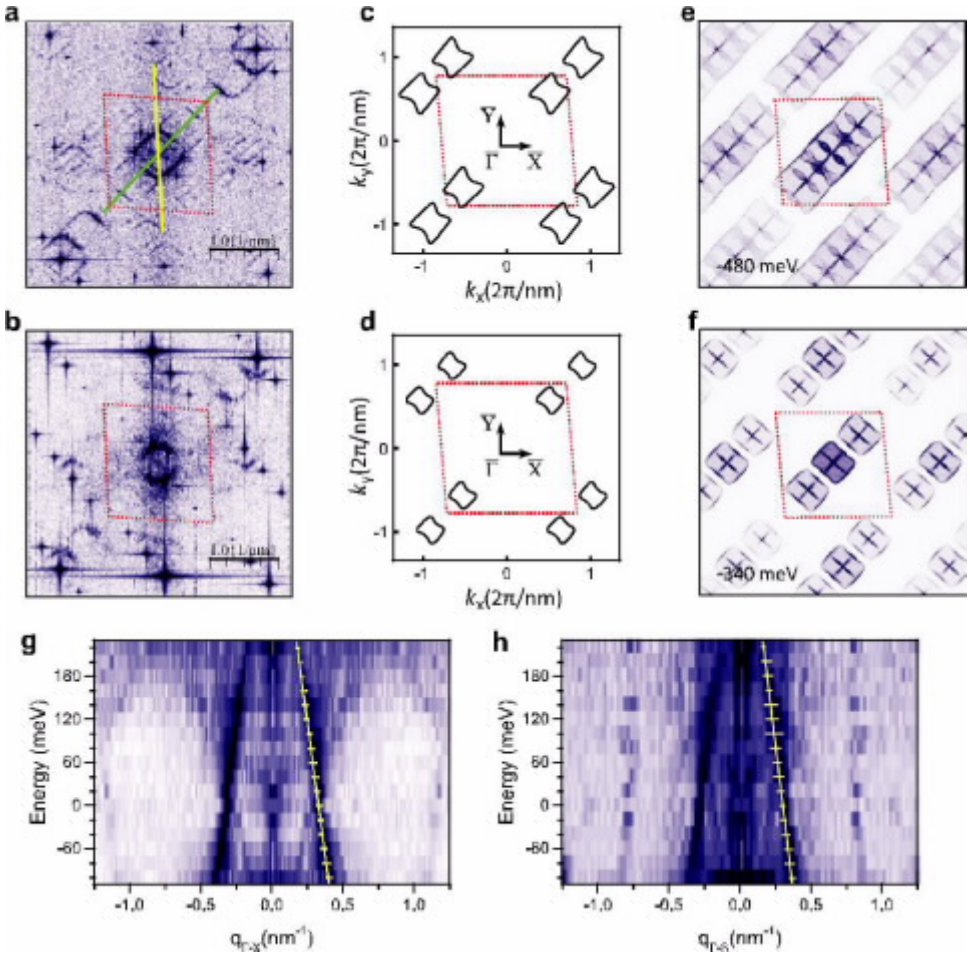


Figure 3. Comparison of experimental and DFT simulated QPI patterns and *E*–*q* dispersion of single-layered α-antimonene. a,b) FFT of experimentally obtained d*I*/d*V* maps taken at *U* −20 and *U* 120 mV. The red dotted squares mark the 1st Brillouin Zone of R2 reconstruction. c,d) DFT calculated CEC for −480 and −340 mV. The high symmetric directions are labeled according to energy band of R2 reconstruction. e,f) The corresponding simulated QPI of (c) and (d). The red square is used to compare with (a) and (b). g,h) *E*–*q* dispersion taken along the yellow (Γ–X) and green (Γ–S) lines in (a). The error bars and linear fitting are included in the right side.

To further explore the band structure of antimonene, QPI is applied to map the dispersive band structure. **Figure 3**a,b shows the fast Fourier transform of two QPI patterns measured on the single layer antimonene at *U* −20 and *U* 120 mV, respectively (more QPI data can be found in Figures S8 and S9, Supporting Information). Besides the static vectors that origi-nated from the R2 reconstruction/moiré pattern, the QPI-asso-ciated pattern can be identified as the square centered at the Γ point. Along the Γ–S direction (the green line in Figure 3a) is located two replicas of the centered square. The diameter of the square becomes gradually smaller with increasing bias energy, (as shown in Figure S9, Supporting Information), indi-cating that it is originated from the hole pocket of Sb valence band. The contribution from the WTe_2 substrate, identified as the two arcs symmetrically located along Γ–X,[49] is rather weak. Therefore, we believe the QPIs are dominated by the con-tribution from the Sb layer. Figure 3c,d shows the calculated constant energy contour (CEC) at −480 and −340 meV below the valence band maximum for the monolayer α-antimonene in R2 reconstruction. The most dominating pattern is two square-shaped pockets located along the Γ–S direction. Taking into account the hole doping effect, the simulated QPI pat-terns as shown in Figure 3e,f are qualitatively consistent with the experimental results of Figure 3a,b. Figure 3g,h shows the *E*–*q* dispersion obtained from the line-cuts taken along the Γ–X and Γ–S direction (yellow and green lines in Figure 3a). Both of the *E*–*q* curves show the linear dispersion, consistent with the DFT-calculated band structure (Figures S7 and S10, Supporting Information). The QPI measurements taken on the bilayer and trilayer antimonene exhibit more complicated patterns, (as shown in Figures S11 and S12, Supporting Information). Whilst, the linear dispersion crossing the Fermi energy can be still distinguished.

The agreement of QPI results with the DFT simulations leads to a conclusion that the epitaxial antimonene holds the similar band structure with the freestanding antimonene. The energy band crossing the Fermi level is linearly dispersed, and thus the small effective mass and high carrier mobility are expected, as theoretically predicted.[50] Simply assuming the isotropic case, the electrical conductivity σ can be described by

© 2018 WILEY-VCH Verlag GmbH & Co. KGaA, Weinheim

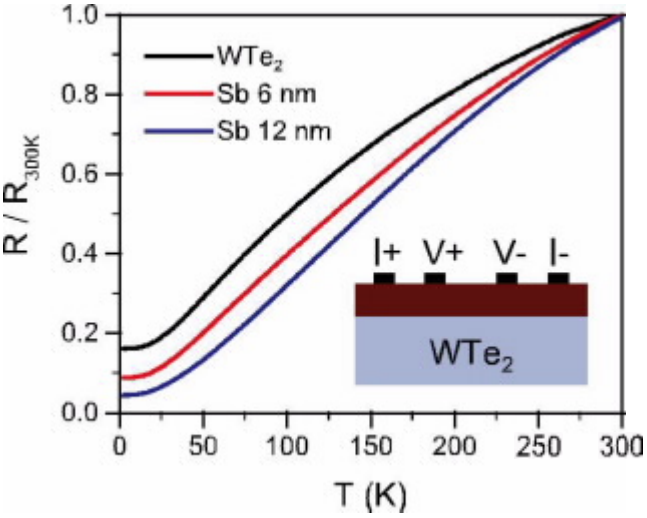


Figure 4. Transport measurement of α-antimonene film. Temperature dependence of longitudinal resistance normalized at 300 K for bare T_d-WTe_2 and α-antimonene films with different thickness. The inset shows the schematic of the four-probe resistance measurement.

the formula of σ ne , where is the carrier mobility, which is inversely proportional to the effective mass, n is the carrier density, and e is the elementary charge. The small effective mass means a high electrical conductivity. To confirm the high elec-trical conductivity, we measure the temperature-dependent resist-ance (R) of α-antimonene films, as plotted in **Figure 4**. Referring to the bare WTe_2, the resistance of WTe_2 coated with ≈10 layers of antimonene film is decreased to nearly a half at the low tempera-ture end. As the antimonene film is grown thicker to ≈20 layers, the resistance is further decreased to about a quarter. Even though it is not possible to extract the resistance of pure antimonene due to the conductive T_d-WTe_2 substrate, the qualitative analysis suggests a good electrical conductivity in α-antimonene film.

Stability is another essential concern considering its prac-tical applications.[46] We investigate the chemical stability of the antimonene film upon exposure to oxygen and air. **Figure 5**a,b shows the multilayered antimonene surface after exposure to oxygen gas of ≈12 000 Langmuir (≈20 min). Other than some adsorbates adsorbed at the surface defective sites, as marked by the arrows in Figure 5b, the surface looks almost the same as before oxygen dosing (Figure 2a). The α-antimonene films are also stable after exposed in air. Figure 5c shows the atomic force microscopy (AFM) image taken after the sample is exposed in air for ≈12 h. The antimonene islands are still kept flat and clean. In contrast, the exposed WTe_2 substrate are covered by small clusters, which may be caused by the surface adsorption.

In summary, the high-quality and large-scale α-antimonene with puckered BP structure has been experimentally realized, thus confirming that it is energetically stable. The linearly dis-persed metallic band leads to the high electrical conductivity. Such advanced properties, together with its chemical inertness under ambient condition and the structural similarity to BP, make it potential in 2D-material-based applications. It is also expected that this study will stimulate further investigation regarding its topological properties or thermal electric applications.

Experimental Section

Sample Growth and STM Characterization: The high quality antimonene films were grown in a combined STM–MBE system (Unisoku USM1500) with a base pressure of 1 10^{-11} Torr. The single crystal T_d-WTe_2 substrate was firstly in situ cleaved in ultrahigh vacuum. The atomic quality of cleaved surface was checked by STM prior to antimonene growth. High purity antimony (alfa Aesar 99.9999%) was evaporated from a standard Knudsen cell. The Sb flux was kept at ≈0.3 monolayers per minute. During the growth, the substrate was kept at ≈400 K. After growth, the antimonene film was transferred to low-temperature STM stage for characterization. All the STM experiments were performed at 4 K with a PtIr tip unless particularly stated. The topographic images were acquired using a constant current mode. The scanning tunneling spectroscopy were acquired with a lock-in amplifier technique. The data were processed with the WSXM software.[51] Oxygen gas was introduced into UHV through a leak valve. The oxygen pressure was kept at 1 10^{-5} Torr during dosing.

DFT Calculations: First-principles calculations were based on DFT by using the Vienna Ab Initio Simulation Package (VASP).[52] The projector-augmented wave (PAW) method[53,54] with a plane wave basis set was used to describe the ion–electron interactions. The exchange-correction potentials were approximated by the generalized gradient approximation (GGA) parameterized by the Perdew–Burke–Ernzerhof (PBE)[55] method. The 2D crystals were modeled by supercells repeated periodically in the 2D plane, while a vacuum region of more than 15 Å was applied to avoid the interactions between the periodic images. Calculations were performed with an energy cutoff of 300 eV on a 12 12 1 Γ-centered Monkhorst–Pack[56] k-point mesh. During structural optimization, the force convergence criterion was set to 0.01 eV $Å^{-1}$. The van der Waals

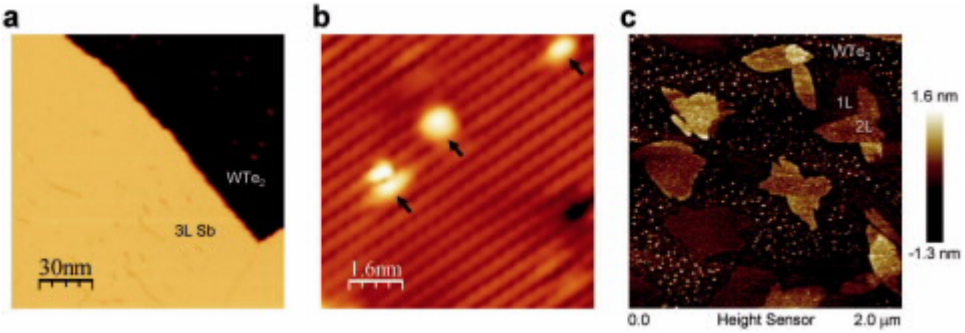


Figure 5. Chemical stability of α-antimonene films upon exposure to O_2 and air. a) The surface morphology (150 150 nm^2) of multilayered antimonene after exposure to pure oxygen gas for ≈12 000 Langmuir. U 2 V, I_t 100 pA. b) Atomically resolved STM image (8.0 8.0 nm^2) of the α-antimonene surface. U 20 mV, I_t 200 pA. The adsorbates are marked by black arrows. c) AFM image taken on the sample after exposure in air for about 12 h.

© 2018 WILEY-VCH Verlag GmbH & Co. KGaA, Weinheim